

## MODELLING THE 3 MICRON REGION IN AKARI IRC SPECTRA

MARK HAMMONDS<sup>1</sup>, TAMAMI MORI<sup>1</sup>, FUMIHIKO USUI<sup>1</sup>, AND TAKASHI ONAKA<sup>1</sup><sup>1</sup>Department of Astronomy, The University of Tokyo, Tokyo 113-0033, Japan*E-mail: hammonds@astron.s.u-tokyo.ac.jp**(Received December 27, 2015; Revised October 21, 2016; Accepted October 21, 2016)*

## ABSTRACT

The existence of polycyclic aromatic hydrocarbons (PAHs) astronomically is well accepted, but the specific molecular forms observed remain uncertain. To better understand the molecular structures which may be present along a given sightline, the 3.0 – 3.6  $\mu\text{m}$  region is modelled with careful consideration given to the underlying sub-features arising from specific structures within emitting molecules.

*Key words:* ISM: H II regions — astrochemistry — infrared: ISM

## 1. INTRODUCTION

The 3.3  $\mu\text{m}$  feature is one of several infrared emission bands in the near to mid-infrared, attributed to the ubiquitously observed polycyclic aromatic hydrocarbons (PAHs) and/or related hydrocarbon species (Tielens, 2008), with some of the best available data in this wavelength range having been recorded by the AKARI space telescope. The 3.3  $\mu\text{m}$  feature was noted by Tokunaga et al. (1991) as having significant variability in peak wavelength position and line profile. An explanation for this phenomenon, proposed by Song et al. (2003), is that the emission band at 3.3  $\mu\text{m}$  is actually composed of two blended sub-features at 3.30  $\mu\text{m}$  and 3.28  $\mu\text{m}$  (see Candian et al. (2012) for a full discussion); they found the 3.3  $\mu\text{m}$  band shows clear evolution in the outflow of HD 44179, observed as a simple Lorentzian profile towards the central star in the object and proceeding to be increasingly broad and asymmetric with offset.

Candian et al. (2012) later confirmed this hypothesis, using integrated field unit (IFU) imaging to show that the 3.28  $\mu\text{m}$  component forms further out in the nebula, becoming strongest only after the 3.30  $\mu\text{m}$  component begins to fall in intensity. Observed in a single object, this implies an evolution of aromatic carbonaceous material. The work presented here aims to explore this idea by incorporating these two features into a new model

for AKARI grism data to investigate whether these two sub-features are present more generally in the interstellar medium (ISM). This may allow more detailed observational analyses of the structures present in specific populations of PAH molecules, and studies on evolution of interstellar carbonaceous material.

## 2. AKARI DATA REDUCTION AND SPECTROSCOPIC MODELLING

AKARI was an extremely successful mission, accomplishing a total of 9813 spectroscopic observations with the Infrared Camera (IRC) instrument during its  $\sim 5$  year productive lifespan. From these observations, a total of 128 targets were selected towards Milky Way ISM regions (such as H II regions and similar infrared sources), primarily distributed across the galactic disk. The spectra of interest are all recorded in grism mode, using the “Ns” ( $0.8' \times 5''$ ) and “Nh” ( $1' \times 3''$ ) slits, with  $R \sim 115$  and  $R \sim 175$  respectively. These targets were chosen from a larger sample of available grism spectra; the selection was narrowed by discarding any data contaminated by instrumental artefacts or excessive ice absorption, together with non-detections of the 3.3  $\mu\text{m}$  band or insufficient signal-to-noise. Data were reduced using the standard IDL pipeline for AKARI IRC Phase 3 data (version 20111121), including additional dark subtraction required to reduce the more pronounced artefacts which often contaminate grism data (Mori et al.,

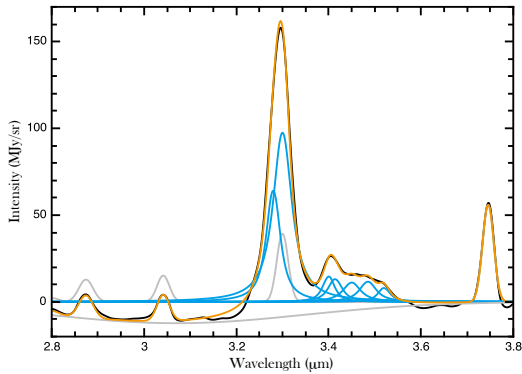


Figure 1. The spectroscopic fitting model used in this work. Original data is shown as the black dot-dashed line (solid black), and the sum of the model is shown in solid gray (orange), hydrocarbon Lorentzian profiles are solid gray (cyan) lines, and background components are shown as gray dashed (gray solid) lines. (Parentheses give colours for the online version.)

2014). Continua were subtracted using a spline function with 3 points chosen in spectroscopic regions expected to be free from any emission or absorption features.

Modelling was performed using the “fityk” software package (Wojdyr, 2010), taking into account several underlying components (the model is shown in figure 1). Background features include Pfund recombination lines due to atomic hydrogen, modelled as gaussian profiles with fixed central wavelengths. Some subtle FWHM variations and central wavelength shifts were noticeable in the data (typically on the order of 0.002 – 0.005  $\mu\text{m}$ , as expected for ISM velocity shifts). This was accounted for by using the Pf $\gamma$  line for calibration. The Pf $\delta$  line at a rest wavelength of 3.297  $\mu\text{m}$  is unresolvable in our data and its intensity was estimated using the adjacent Pf $\gamma$  and Pf $\epsilon$  lines, with Case B calculations (assuming  $T = 10^4$  K and  $n = 10^4$   $\text{cm}^{-3}$ ) as described by Hummer & Storey (1987). In addition, the fit for some objects was improved by the addition of a small feature at 3.235  $\mu\text{m}$ , corresponding to the H<sub>2</sub> (O5) line. This feature is detectable in only a few sources of sufficiently high signal-to-noise and does not appear to make a significant contribution to the overall profile of the 3.3  $\mu\text{m}$  band.

### 2.1. Hydrocarbon Emission Features

All hydrocarbon emission features are modelled as Lorentzian profiles, with fixed central wavelengths of 3.28, 3.30, 3.40, 3.414, 3.45, 3.485, and 3.52  $\mu\text{m}$ , compa-

table with previous assignments of features in the 3.3 – 3.6  $\mu\text{m}$  region (see, *e.g.* Gadallah et al (2012) for further discussion). FWHM was left as a separate free parameter for each profile to allow for, *e.g.*, line broadening due to temperature or solid state effects. These allowances are to account for band carriers potentially arising from different chemical and physical environments, which may cause varying degrees of line broadening. Contrary to some previous attempts to model this region, no underlying plateau was used below the 3.3  $\mu\text{m}$  band, allowing for a more straightforward model where the wings from the main Lorentzian components account for the observed “plateau”. The addition of two features at 3.40  $\mu\text{m}$  and 3.414  $\mu\text{m}$  is necessary to account for the observed asymmetry in the 3.4  $\mu\text{m}$  aliphatic band, and is consistent with the two aliphatic C–H stretches expected in this region. Inclusion of two sub-features to model the 3.3  $\mu\text{m}$  band allows a much more accurate match for the observed band profile.

### 2.2. Ice Absorption Feature

The ice absorption feature centred at 3.07  $\mu\text{m}$  is observed in a majority of sightlines. Its profile is challenging to match due to its asymmetric red-degraded tail, the cause of which is not well understood. This causes some overestimation of the continuum around 3.2  $\mu\text{m}$  and 3.6  $\mu\text{m}$  which is noticeable but within error. A full description of the ice feature profile would be beneficial for future studies of both ice and hydrocarbons, but is outside the scope of this work. Therefore, a single function description is used here. Given the broad nature of the ice feature and neglecting the left edge of the absorption profile (which is not relevant to this work), intensities predicted for the deconvolved hydrocarbon emission features are not significantly affected by the type of function used. Using a Lorentzian profile instead of a Gaussian profile causes predicted values to be slightly higher but still within error. Variation increases with offset from the central wavelength of 3.07  $\mu\text{m}$ . In the example spectrum of IRAS 12073-6233 the ratio of intensities  $I_{(3.28)}/I_{(3.30)}$  is 0.689, 0.692, and 0.692 for Gaussian, Lorentzian, and Voigt absorption profiles respectively.

## 3. CONCLUSIONS

This work verifies the two component (3.28  $\mu\text{m}$  and 3.30  $\mu\text{m}$ ) interpretation of the 3.3  $\mu\text{m}$  band observed astronomically. In all AKARI data examined, this model provides a close match for the observed data,

allowing the entire band to be easily modelled with a series of Lorentzian functions without an underlying plateau feature. The variation in the profile of the 3.3  $\mu\text{m}$  band suggests that the 3.28  $\mu\text{m}$  carrier is present in varying amounts, dependent on astrophysical environment. While Figure 1 shows a typical example spectrum, the ratio of  $I_{3.28}/I_{3.30}$  across the galactic disk is found to vary from 0.2 and 2.2, with a significant number of points being close to unity. Therefore, the relative strength of this component suggests that PAH structures which give rise to 3.28  $\mu\text{m}$  emission may make a significant contribution to the observed emission, and should be given greater consideration in efforts to model interstellar species.

#### ACKNOWLEDGMENTS

With thanks to Helen Fraser, Kirstin Doney, and Ronin Wu for helpful discussions. This work is supported by a Grant-in-Aid for Japan Society for the Promotion of Science (JSPS) fellows. This research is based on observations with AKARI, a JAXA project with the participation of ESA.

#### REFERENCES

- Candian, A., Kerr, T. H., Song, I. -O., McCombie, J. and Sarre, P. J., 2012, Spatial distribution and interpretation of the 3.3  $\mu\text{m}$  PAH emission band of the Red Rectangle, *MNRAS*, 426, 389.
- Gadallah, K. A. K., Mutschke, H. and Jäger, C. 2012, Mid-infrared spectroscopy of UV irradiated hydrogenated amorphous carbon materials, *A&A*, 544, A107.
- Hummer, D. G. and Storey, P. J., 1987, Recombination-line intensities for hydrogenic ions. I - Case B calculations for H I and He II, *MNRAS*, 224, 801.
- Mori, T. I., Onaka, T., Sakon, I., Ishihara, D., Shimonishi, T., Ohsawa, R. and Bell, A. C., 2014, Observational Studies on the Near-infrared Unidentified Emission Bands in Galactic H II Regions, *ApJ*, 784, 53.
- Song, I. -O., Kerr, T. H., McCombie, J., & Sarre, P. J., 2003, Evolution of the 3.3- $\mu\text{m}$  emission feature in the Red Rectangle, *MNRAS*, 346, L1.
- Tielens, A. G. G. M., 2008, Interstellar Polycyclic Aromatic Hydrocarbon Molecules, *Annu. Rev. A&A*, 46, 289.
- Tokunaga, A. T., Sellgren, K., Smith, R. G., Nagata, T., Sakata, A., & Nakada, Y. 1991, High-resolution spectra of the 3.29 micron interstellar emission feature - A summary, *ApJ*, 380, 452.
- Wojdyr, M. 2010, Fityk: a general-purpose peak fitting program, *J. App. Cryst.*, 43, 1126.